

Performance of Next-Generation Cellular Networks Guarded with Frequency Reuse Distance

Akram Al-Hourani, *Senior Member, IEEE*, and Martin Haenggi, *Fellow, IEEE*

Abstract—In this paper we lay an analytic framework for computing the downlink success probability of cellular networks, taking into account a frequency reuse distance as an interference mitigation scheme. We model the frequency reuse distance using tools from stochastic geometry, namely, we utilize the Matérn hard-core (MHC) point process to capture the effect of interference protection zones created around base stations. To model the overall cellular network, we introduce a new point process composed of N superimposed MHC processes, where each individual MHC process corresponds to a co-channel base station group; this new point process is called the union-MHC (UMHC) process. We further investigate the resulting performance of the UMHC process and present the link success probability in integral form. The success probability can be evaluated for an arbitrary fading model and an arbitrary number of orthogonal resource groups. We test the newly proposed model against practical data sets from a network operator and observe a good match of the results.

Index Terms—Cellular networks, stochastic geometry, Matérn hard-core process, frequency reuse.

I. INTRODUCTION

THE vast deployment of cellular networks resulted in a ubiquitous infrastructure around the world, which is still continuously expanding at an accelerating pace. The strategic planning of such networks arises as an important aspect that guarantees market competency and copes with the rapid increase in traffic demand. Network operators resort to extensive simulations to draw a rough estimate of the cellular performance under future demand assumptions. These simulations are usually scenario-specific, tailored for a certain layout and configuration. Furthermore, the emerging self-organizing features in 5G networks make the traditional planning techniques less accurate [1], due to the vast configuration possibilities that a network can take during the course of its evolution.

Theoretical methods, on the other hand, are based on analytic and mathematical models to predict the network performance based on different encircling probabilistic conditions. Analytic models can provide a direct relation between these conditions and the predicted network performance [2]. That is, in contrary to simulation methods that are not intended to provide mathematical tractability.

One of the main uncertainties in wireless networks lies in the location of users and the location of base stations

(BSs). The irregularity of the location of users is due to the mobility and the natural randomness of human behavior, while the irregularity of BS locations can be attributed to many factors such as the urban structures, availability of utilities, building/urban planning codes and other geoeconomic factors. From this perspective, stochastic geometry is an effective tool to capture the intrinsic randomness in the geometry of cellular networks, and the popularity of this technique is increasingly expanding among researchers.

In stochastic geometry, a point process (a random set of points) is used to model the distribution of cellular base stations. The Poisson point process (PPP) is a popular choice by many researchers due to its tractability and simplicity, facilitated by a rich set of theoretical results [3].

Many works have been based on PPP to develop tractable approaches for describing interference, success probability, and rate of cellular networks [3]–[7]. The points in a PPP do not exhibit correlation, i.e., the location of a point does not influence the locations of other points. Thus when using a PPP, an overestimation in the co-channel interference usually occurs as a result to the possible extreme proximity of points. Accordingly, the PPP produces lower bounds of the performance metrics [8] when the actual base stations positions exhibit repulsion. Alternative methods to represent the natural repulsion of base stations are utilized by [9], [10] using less tractable point processes such as the suggested β -Ginibre point process. However, the relation between the theoretical repulsion parameter and the actual frequency reuse distance is not established.

In actual cellular networks, interference mitigation schemes are usually applied to increase the link success probability. These schemes are all centered around the orthogonal use of radio resources in one (or multiple) of the spatial-temporal-spectral domains. Modeling these schemes is not a trivial exercise due to the convoluted relation between the location of users, traffic load, and the arising mutual interference. Simplified approaches to theorize the reuse of an arbitrary number of temporal-spectral resources are presented in multiple places [11], [12] by assuming a random reuse pattern, thus performing a random *thinning* on a PPP, which greatly facilitates the tractability, because the random thinning of a PPP yields simply another PPP of a reduced density [3].

Hard-core point processes, on the other hand, prohibit co-channel transmitters (points) from co-existing closer than a predefined distance called the *hard-core distance*; these processes are previously used to model concurrent transmitters in CSMA networks [13]–[15]. Similarly, in this paper we utilize the Matérn hard-core (MHC) point process of type II

A. Al-Hourani, is with the School of Engineering, RMIT University, Melbourne, Australia. E-mail: akram.hourani@rmit.edu.au

M. Haenggi is with the Department of Electrical Engineering, University of Notre Dame, Indiana, USA. E-mail: mhaenggi@nd.edu

The work was supported in part by the US National Science Foundation (grant CCF 1525904).

[3, Def. 3.8] to capture the effect of resource-reuse schemes in cellular networks. Accordingly, we derive the statistical behavior of the interference originated from a field of MHC base stations interfering at a mobile user located at a certain distance from its serving BS. Then we employ this statistical behavior to calculate the downlink success probability of the overall cellular network. The main contributions of this paper are:

- We provide a novel model to represent frequency reuse in cellular networks using a superposition of MHC point processes.
- We provide an approximation for the statistics of the downlink interference on a cellular user generated by base stations using a frequency reuse distance.
- We present a general formula to calculate the success probability in cellular networks guarded with frequency reuse scheme.
- We provide a comparison with real-world data to verify the accuracy of the provided analytic model.

For convenience, we list in Table I the main mathematical symbols and notations.

II. BACKGROUND AND RELATED WORK

The utilization of stochastic geometry in modeling cellular networks has long been investigated by the research community. References to this subject are numerous, with a vast trend of adapting the PPP for modeling the spatial distribution and Rayleigh distribution for modeling the channel fading process [16]. These two assumptions can greatly facilitate tractability and mathematical derivations. On the other hand, the use of general fading models is less popular due to its computational complexity [17], [18] although it provides more accurate modeling for wireless cellular networks.

Traditionally, in some previous generations of mobile networks (e.g., 2G), a good frequency-plan was achieved via extensive planning-optimization cycles, where both manual and automated engineering efforts were essential in this process. In contrast, in recent and future cellular network generations (4G and 5G), a universal frequency reuse factor is adopted, where all base stations have access to the same pool of frequency bands¹. The hustle of manual frequency-plan iterations is left to fully-automated real-time coordination between base stations that dynamically allocates resources based on traffic load. In spite of this great interference coordination capability of modern cellular networks, researchers widely adopt a randomized frequency assignment model (see [19] and references therein). The reason is that a randomized frequency plan preserves the properties of PPP and thus its tractability at the cost of reducing the accuracy of the model. Accordingly, when using the PPP model, the aim is more focused on establishing the performance bounds rather than producing a tight replication of experimental measurements.

While more accurate modeling of interference mitigation is proposed in the literature [13]–[15], [20], [21] for capturing

¹A widely adopted 3G system is based on the UMTS standard which utilizes a code-division multiple access scheme. This multiple access scheme does not permit a granular assignment of the spectrum.

random spectrum access, these models are more suitable for wireless sensor networks and CSMA networks. To model interference coordination, one can exploit the repulsion property in *hard-core point processes*, a subclass of *repulsive point processes*. Thus, a thinned process based on the hard-core distance can emulate an interference protection zone around every node in the network and thus reduces the interference.

Several other point processes were proposed in the literature to model the geometry of the cellular network, mainly targeting the dependent deployment of femto-cells in the presence of macro-cells. In this type of heterogeneous deployments, femto-cells are usually deployed in a hot-spot manner following the concentrated pockets of users. The work in [22] assumes that femto-BSs are randomly deployed where macro-BSs are absent, thus aiming to patch the coverage gaps left by the macro-BSs. This scheme is a direct utilization of the Poisson hole process (PHP) [23].

Soft-core point processes also belong to the class of repulsive point processes. The works in [9], [10], [24] utilize the β -Ginibre process, which has an adjustable parameter $\beta \in (0, 1]$ to capture the degree of repulsion between the locations of the base stations. The work in [25] puts forth a general framework for non-Poisson networks including the β -Ginibre point process; the paper proposes an analytically grounded and justified approximation method to calculate the network performance based on the tractable formulae of the PPP by shifting the SIR distribution.

In contrast to soft-core point processes, the points in hard-core point processes are strictly banned from co-existing closer than the hard-core distance. The MHC process belongs to the hard-core family and was used in the context of cellular networks in [26] providing lower bounds of the success probability using Jensen's inequality. However the analysis does not present an explicit formula for the interference, utilizes a rough approximation to the contact distance, and is restricted to Rayleigh fading only.

The main novelty in this paper is that it analyzes the success probability and the downlink interference statistics of a superposition of MHC point processes. This superposition models both the spatial and logical distribution of cellular base stations, where co-channel base stations are modeled in a single MHC process and the overall geometrical distribution is captured by the superposition. This approach is shown to capture actual network deployments much more accurately than random frequency reuse in PPPs.

III. NETWORK MODEL

In this section, we construct the mathematical model that emulates the downlink interference of cellular base stations on mobile users. It is important to note in the case of LTE (and its extension to 5G), although the reuse factor of the entire bandwidth is unity, OFDM resource blocks are dynamically assigned and negotiated between nearby base stations depending on the traffic load distribution. This is indeed a major advantage over GSM where channels were statically

assigned².

The concept of avoiding co-channel interference in LTE is based on assigning orthogonal resource blocks to cellular users to avoid potential interference. This mechanism can still be seen, in principle, as frequency-reuse, where the geometrical proximity plays the major role in determining potential interfering channels.

Hard-core point processes prohibit points to be closer than a certain distance δ called the *hard-core distance*. This property can be utilized to model the interference protection zone, within which BSs are prohibited from assigning the same radio resources in the downlink.

One of the main hard-core point processes is the Matérn hard-core (MHC) point process type II, introduced in [27]. To construct this process, we start from a homogeneous PPP denoted as Φ_b (called the *base process*) of intensity λ_b , then we mark each point independently with a uniform random variable, i.e., $m_x \sim \mathcal{U}(0, 1)$. After that, for each point x , we check within the ball $b(x, \delta)$ for any other point having a lower mark than x . If we find such a point, then x is flagged for removal. The final step is to remove all points that were flagged. The resulting MHC point process is denoted as Φ and can be expressed as follows [3, Def. 3.8],

$$\begin{aligned} \Phi &\triangleq \{x \in \Phi_b : m_x < m_y, \forall y \in \Phi_b \cap b(x, \delta) \setminus \{x\}\}, \\ &\triangleq \text{MHC}(\Phi_b), \end{aligned} \quad (1)$$

where $\text{MHC}(\cdot)$ is the dependent thinning operator. It can be easily shown that the resulting intensity of Φ is given by [28]

$$\lambda_{\text{MHC}} = \rho \lambda_b = \frac{1 - \exp(-\pi \delta^2 \lambda_b)}{\pi \delta^2}, \quad (2)$$

where ρ is the retention probability of the points in the base PPP.

We call the resulting point process of superimposing multiple i.i.d. MHC processes as the *Union-MHC* (UMHC). Formally, we define the UMHC process as

$$\Xi \triangleq \bigcup_{i=1}^N \Phi^{(i)}, \text{ where } \Phi^{(i)} = \text{MHC}(\Phi_b^{(i)}). \quad (3)$$

Its intensity is

$$\lambda_{\text{UMHC}} = N \lambda_{\text{MHC}}. \quad (4)$$

In this paper we represent the location of base stations using a UMHC process, where each element process $\Phi^{(i)}$ represents a co-channel base station group (also called a *resource group*), since they share the same radio resources and are logically having the same *color*³. Note that in practice, a resource group is composed of base stations using non-orthogonal radio resources and are mutually interfering. We depict a realization of a UMHC process in Fig. 1 for $N = 3$ resource groups, indicating the interference protection zone around BSs of the first resource group as an example.

²In GSM, a frequency hopping scheme might be enabled, however this does not change the fact that the number of channels is constant in a given cell depending on the number of available transceiver (TRX) modules.

³More precisely, a *color* represents the BSs that are using the same resource block (RB). BSs with different colors are considered non-interfering

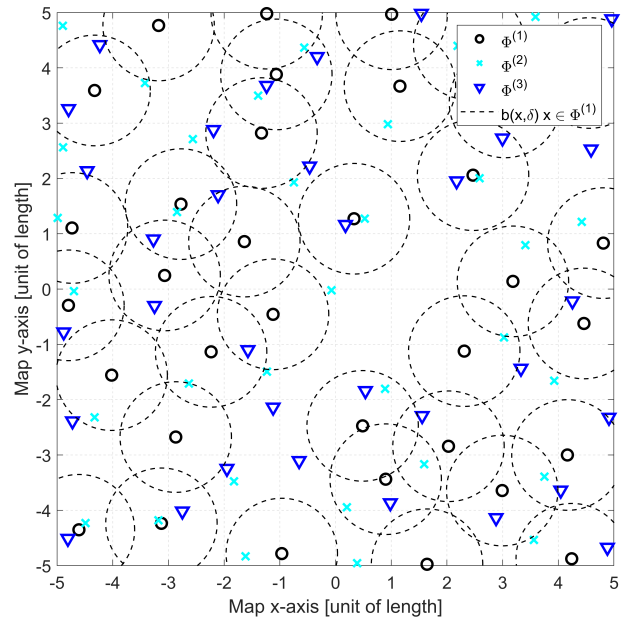


Fig. 1. A realization of a UMHC point process with $N = 3$, $\delta = 1$ and $\lambda_{\text{MHC}} = 1/\pi$, indicating the hard-core zones of the first element process $\Phi^{(1)}$.

TABLE I
NOTATIONS AND SYMBOLS

Symbol	Explanation
Φ_b	PPP (the base process)
Φ	MHC point process
Ξ	UMHC point process
$\text{MHC}(\cdot)$	MHC thinning operator
λ_b	The parent PPP intensity
λ_{MHC}	MHC intensity
λ_{UMHC}	UMHC intensity
δ	Hard-core distance (frequency reuse distance)
m_x	The mark of point x
ρ	Unconditional MHC retention probability
N	The number of resource groups (colors)
$g(r)$	Pair correlation function for isotropic point process
$\varrho^{(2)}(r)$	Second moment density
$k(r)$	The probability of two points in the base PPP separated by distance r to be both retained
R_o	Contact distance random variable
ϕ	The angle between an interfering BS and the serving BS
h	Channel fading random variable
h_o	Channel fading of the serving BS
α	Path loss exponent
θ	SINR service threshold

IV. UMHC PROPERTIES

In order to study the plausibility of utilizing the UMHC process to represent cellular networks, we investigate its regularity by examining its pair correlation function. If this function is equal to unity, then the points have no pairwise correlation in their locations, while values less than unity indicates a *repulsive* behavior between points and vice-versa for *clustering*. The pair correlation function for a motion-invariant process is defined as [3]

$$g(r) \triangleq \frac{\varrho^{(2)}(r)}{\lambda^2}, \quad (5)$$

where λ is the intensity, and $\varrho^{(2)}(r)$ is the second moment density, which can be informally understood as the joint probability that there are two points separated by the distance r [3].

Lemma 1. *The pair correlation function of the UMHC process is given by*

$$g_{\text{UMHC}}(r) = \frac{k(r)}{N} \frac{\lambda_b^2}{\lambda_{\text{MHC}}^2} + \frac{N-1}{N}. \quad (6)$$

where $k(r)$ is the probability of two points in the parent PPP separated by a distance r to be both retained in the resulting MHC process [29]. It is given by [13]

$$k(r) = \begin{cases} 0 & r < \delta \\ 2 \left(\frac{1 - e^{-\pi \delta^2 \lambda_b} + e^{-\lambda_b V(\delta, r)} - 1}{\pi \delta^2} \right) \frac{V(\delta, r)}{\lambda_b^2 (V(\delta, r) - \pi \delta^2)} & r \geq \delta, \end{cases} \quad (7)$$

where

$$V(\delta, r) = \begin{cases} 2\pi \delta^2 - 2 \cos^{-1} \left(\frac{r}{2\delta} \right) \delta^2 + \sqrt{\delta^2 - \frac{r^2}{4}} r & r \leq 2\delta \\ 2\pi \delta^2 & r > 2\delta \end{cases} \quad (8)$$

is the union area of two disks of radius δ whose centers are separated by a distance r .

Proof. We start from the second moment density of a single MHC point process given as [29]

$$\varrho_{\text{MHC}}^{(2)}(r) = \lambda_b^2 k(r). \quad (9)$$

Similarly, by considering the union of all the N parent PPPs, we can think of the event of retaining both points as the union of the following two mutually exclusive cases: (i) the points belong to the same parent PPP, which occurs with a probability $\frac{1}{N}$; in this case, the retention probability is $k(r)$, and (ii) the points belong to two different parent PPPs, which occurs with probability $1 - \frac{1}{N}$; in this case the retention probability is $\rho^2 = \left(\frac{\lambda_{\text{MHC}}}{\lambda_b} \right)^2$. The retention probability in the second case is ρ^2 because each point is independently retained with probability ρ as the points belong to two independent PPPs. Accordingly, we express the two-point retention probability of the UMHC process as

$$k_{\text{UMHC}}(r) = \underbrace{\left(\frac{1}{N} \right) k(r)}_{\text{Case(i)}} + \underbrace{\left(1 - \frac{1}{N} \right) \left(\frac{\lambda_{\text{MHC}}}{\lambda_b} \right)^2}_{\text{Case(ii)}}. \quad (10)$$

Using the definition in (5) we have

$$g_{\text{UMHC}}(r) = \frac{\varrho_{\text{UMHC}}^{(2)}(r)}{\lambda_{\text{UMHC}}^2} = \frac{\varrho_{\text{UMHC}}^{(2)}(r)}{(N\rho\lambda_b)^2}, \quad (11)$$

where the second moment density can be formulated similar to (9), namely

$$\varrho_{\text{UMHC}}^{(2)}(r) = (N\lambda_b)^2 k_{\text{UMHC}}(r). \quad (12)$$

By substituting in (11) we obtain the result of this lemma. \square

Corollary 1. *The pair correlation function of the UMHC process asymptotically tends to unity as the number of the generating parent processes $N \rightarrow \infty$.*

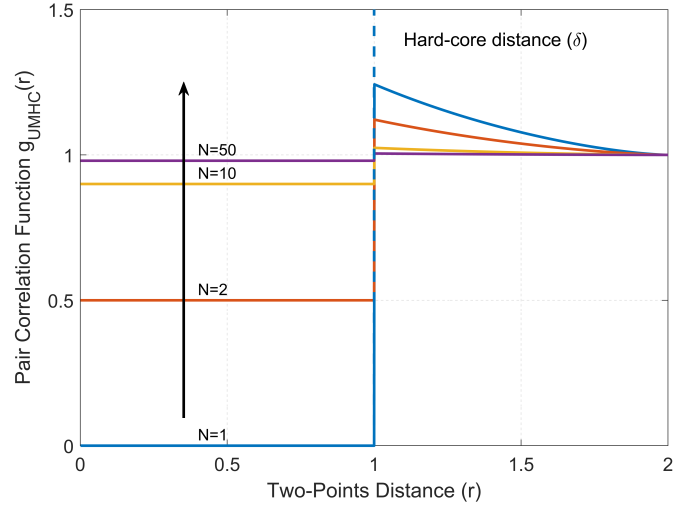


Fig. 2. The pair correlation function of the UMHC point process, indicating the regularity with respect to different number of superimposed processes. $\delta = 1$ and $\lambda_{\text{MHC}} = 1/\pi$.

Proof. For $N \rightarrow \infty$, we have from (6)

$$g'_{\text{UMHC}}(r) = \lim_{N \rightarrow \infty} g_{\text{UMHC}}(r) = 1, \quad r > 0, \quad (13)$$

indicating that the location of the points of the UMHC process become pair-wise uncorrelated. The result also follows from the fact that the superposition of N independent stationary and ergodic point processes approaches a PPP as $N \rightarrow \infty$ [3], [30]. \square

In order to get insights on the transition behavior of the regularity (from a repulsive process to a completely random process), we plot the pair correlation function of the UMHC process in Fig. 2, using infinite parent points intensity of $\lambda_b \rightarrow \infty$ and a hard-core distance $\delta = 1$. As real cellular networks exhibit a certain degree of repulsion between BSs, naturally a suitable analytical model must be repulsive, ideally with an adjustable degree of repulsion. As it can be noted from Fig. 2, the UMHC features this property.

So far, we have shown that increasing the number of parent processes N leads to more randomness in the resulting union of the children processes. Accordingly, for a large N , the UMHC process can be thought as a PPP divided uniformly at random into N groups of points. These groups represents the co-channel base stations.

The particular value of the generating intensity λ_b is irrelevant when modeling a cellular network model, but what matters is the resulting MHC process intensity λ_{MHC} as it will have a direct effect on the interference statistics. Thus, a simplified method to model cellular networks using UMHC point process is to generate the underlying MHC processes using an infinite intensity for the parent point process, i.e., letting $\lambda_b \rightarrow \infty$. The resulting MHC process intensity can then be calculated from the simple relation

$$\lambda'_{\text{MHC}} = \lim_{\lambda_b \rightarrow \infty} \frac{1 - \exp(-\pi \delta^2 \lambda_b)}{\pi \delta^2} = \frac{1}{\pi \delta^2}. \quad (14)$$

Accordingly, a simple relation can be formed to link the reuse distance δ and the number of resource groups N as follows,

$$\delta = \sqrt{\frac{N}{\pi \lambda'_{\text{UMHC}}}}, \quad N \in \mathbb{N}. \quad (15)$$

This relation is deduced by substituting (14) in (4), where λ'_{UMHC} is the overall density of the cellular base stations. Thus, if we have a given number of resource groups N and a given base stations density, then we can calculate the required reuse distance δ to construct the corresponding UMHC model.

A. Contact Distance in UMHC Process

A very important aspect to analyze in a point process model is the contact distance between a mobile user and its nearest serving base station. The statistics of this distance heavily influences the signal strength and the signal-to-interference-and-noise ratio (SINR). We utilize the mathematical framework developed in [28] in order to calculate the distribution of the contact distance between a user placed at the origin and an MHC process (representing base stations), where equations (2) and (15) in [28] yield

$$F_{\text{MHC}}(r) = 1 - \exp\left(-\int_0^r \frac{1 - \exp[-\lambda_b(\pi\delta^2 - l(v, \delta))]}{\pi\delta^2 - l(v, \delta)} 2\pi v \, dv\right), \quad (16)$$

representing the cumulative distribution function (CDF) of the contact distance in a single MHC process, where $l(r, \delta)$ is the area of the asymmetrical lens formed by the intersection of two circles separated by a distance r , one with radius r and the other with radius δ . This area is given by

$$l(r, \delta) = \begin{cases} \pi r^2, & 0 < r < \frac{\delta}{2} \\ r^2 \cos^{-1}\left(1 - \frac{\delta^2}{2r^2}\right) + \delta^2 \cos^{-1}\left(\frac{\delta}{2r}\right) - \frac{1}{2}\delta\sqrt{4r^2 - \delta^2}, & r \geq \frac{\delta}{2}. \end{cases}$$

When multiple MHC processes are superimposed, the user will opt to contact the closest base station of all the superimposed processes. Thus for the typical user at the origin, the contact distance to a UMHC process is given by

$$R_o = \min_{i \in \{1, \dots, N\}} \|\Phi^{(i)}\|. \quad (17)$$

Accordingly, the distribution of the contact distance of the UMHC is

$$F_{\text{UMHC}}(r) = 1 - [1 - F_{\text{MHC}}(r)]^N, \quad (18)$$

because all underlying contact distances are i.i.d.

The form of (16) is somewhat complicated, since it involves an integral over trigonometric functions. Alternatively we could exploit the convergence property of UMHC process to PPP as the number of the superimposed MHC processes increases, thus the contact distance distribution of the UMHC process converges to the simple form of the PPP contact distance, i.e.,

$$F_{\text{PPP}}(r) = 1 - \exp(-\pi \lambda'_{\text{UMHC}} r^2). \quad (19)$$

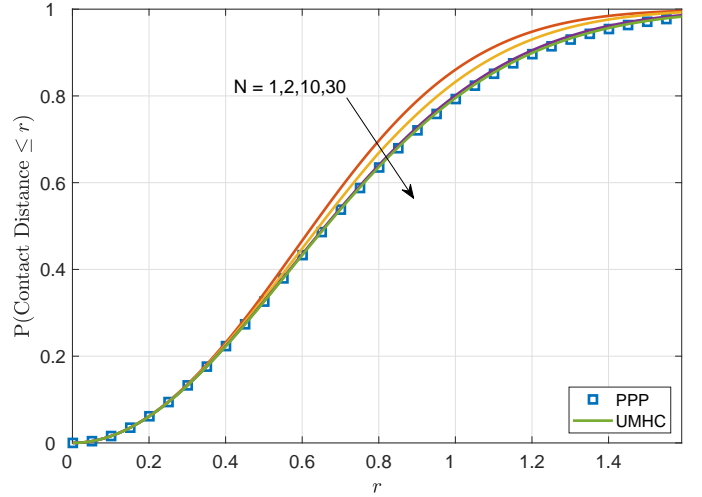


Fig. 3. The asymptotic behavior of the CDF of the contact distance in the UMHC process as per (18), converging to the PPP contact distance described in (19). The parameters are $\lambda_{\text{UMHC}} = 0.3$, $N = \{1, 2, 10, 30\}$, $\lambda_b \rightarrow \infty$.

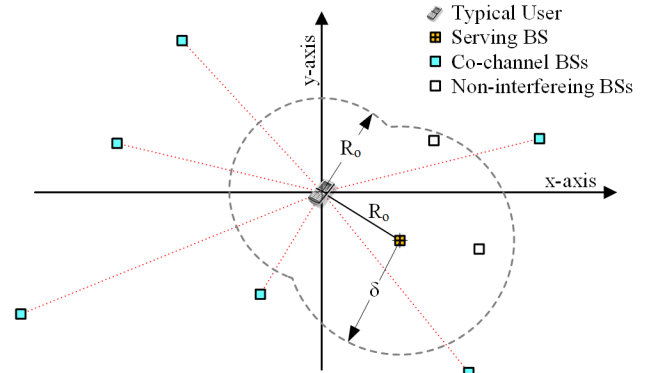


Fig. 4. The interference-free region \mathcal{V} as the union of the two balls $b(x, R_o)$ and $b(u_o, \delta)$.

We depict in Fig. 3 a visualization of the convergence in distribution of the contact distance towards the PPP as per (18) and (19); to establish a valid comparison base in Fig. 3, we consider a constant UMHC intensity λ_{UMHC} , in which the underlying MHC processes are generated based on the given number of resource groups N where that the hard-core distance δ is calculated as per (15). The comparison is made with PPP having an intensity equal to that of the UMHC process, i.e., λ_{UMHC} .

B. Channel Model

We model the mean path loss using the common power-law relation given by $R_u^{-\alpha} = \|u-x\|^{-\alpha}$, where u is the location of the BS, while x is the location of the user, $\|\cdot\|$ is the Euclidean distance, and α is the path loss exponent. The effect of fading on the channel gain is captured in the random variable h . Accordingly the resulting received power from a BS at u is $P_{\text{RX}_u} = h_u R_u^{-\alpha}$, where all BS are assumed to transmit at a common normalized power and the fading process is i.i.d.

V. INTERFERENCE CHARACTERIZATION

Without loss of generality, we consider the typical user at the origin. More precisely, the origin is the typical location we focus on. Also, we assume that a cellular user associates with the closest base station⁴ (called the *serving base station* and denoted as u_o), where,

$$u_o = \operatorname{argmin}\{x \in \Xi: \|x\| < \|y\| \forall y \in \Xi \setminus \{x\}\}, \quad (20)$$

and we denote the distance towards this serving u_o as $R_o = \|u_o\|$ and the resource group of this cell as κ , i.e., $u_o \in \Phi^{(\kappa)}$, and $\Phi_o^{(\kappa)} = \Phi^{(\kappa)} \setminus \{u_o\}$ is the set of co-channel base stations under consideration.

All other *co-channel* BSs, other than the serving one, are considered as interferers. Thus the aggregated interference power at the receiver is

$$I = \sum_{u \in \Phi_o^{(\kappa)}} h_u R_u^{-\alpha}, \quad (21)$$

where R_u is the distance toward the interfering BSs, and h_u are the power fading random variables of the interfering BSs. A key property of the cellular network model is that all interferers are located outside the ball $b(x, R_o)$ since the serving base station is the closest to the user x .

If the co-channel base stations are modeled using a MHC process, there is an interference protection zone around every base station, within which no two co-channel base stations are allowed to co-exist. Thus, all interferers are also outside the ball $b(u_o, \delta)$. As a result, the overall interferer-free region is the union of the two balls $\mathcal{V} = b(o, R_o) \cup b(u_o, \delta)$. Note that when $R_o \leq \frac{\delta}{2}$ where the union, i.e., the interference protection zone, consists only of $b(u_o, \delta)$. The interference-free region is depicted in Fig. 4.

Coming back to the aggregated interference in (21), our aim is to characterize its statistical behavior, ideally by describing its CDF. Unfortunately the CDF of the interference cannot be obtained in a closed form; however, we can still obtain its Laplace transform (LT) $\mathcal{L}_I(s)$, where the LT for a random variable X is defined as $\mathcal{L}_X(s) = \mathbb{E}[e^{-sX}]$, and s is a complex variable. With the LT available, we can utilize a numerical inversion method to compute the CDF of I according to

$$F_I(x) = \mathcal{L}^{-1} \left[\frac{1}{s} \mathcal{L}_I(s) \right]. \quad (22)$$

The particular method we will use in the subsequent numerical examples is called *Talbot Inversion* along with the unified numerical inversion framework developed in [31].

To this end, and in order to find the Laplace transform of the interference, we utilize a similar method as in [4], which considers the interferers to be scattered in the entire plane \mathbb{R}^2 . The difference is that in our approach the distribution of the interferers is restricted to the outside of the interference exclusion region $\mathcal{V} = b(o, R_o) \cup b(u_o, \delta)$.

⁴Note that in practical implementation of cellular networks in urban environment, the shape of the *serving* region of a cell can be discontinuous and patchy. However, the chief goal here is to construct an analytic framework that creates a balance in the trade-off between the insightful formulation and high-accuracy modeling.

Proposition 1. *The conditional Laplace transform given R_o of the aggregated interference of co-channelled BS modeled as a MHC process is approximated by*

Proof. We start from the definition of the Laplace transform of the interference random variable, where the expectation should be performed over (i) the stochastic processes of the radio channel h_u and (ii) over the geometrical stochastic process of $\Phi_o^{(\kappa)}$

$$\begin{aligned} \mathcal{L}_{I|R_o}(s) &= \mathbb{E} \left[e^{-sI} \mid R_o \right] \\ &= \mathbb{E} \left[\exp \left(-s \sum_{u \in \Phi_o^{(\kappa)}} h_u R_u^{-\alpha} \right) \mid R_o \right] \\ &= \mathbb{E} \left[\prod_{u \in \Phi_o^{(\kappa)}} \exp(-s h_u R_u^{-\alpha}) \mid R_o \right] \\ &\stackrel{(a)}{=} \mathbb{E} \left[\prod_{u \in \Phi_o^{(\kappa)}} E_h \left[\exp(-s h_u R_u^{-\alpha}) \mid R_o \right] \right] \\ &\stackrel{(b)}{=} \mathbb{E} \left[\prod_{u \in \Phi_o^{(\kappa)}} \mathcal{L}_h[-s R_u^{-\alpha}] \mid R_o \right], \end{aligned} \quad (25)$$

where (a) stems from the fact that the channels h are independent of the point process and that all h_u are i.i.d. random variables, while (b) follows directly from the definition of the Laplace transform, with R_u given by

$$R_u = \sqrt{r_u^2 + R_o^2 + 2r_u R_o \cos \phi_u}, \quad (26)$$

where $r_u = \|u - u_o\|$ is the distance between the interfering base stations u and the serving base station u_o . The geometrical reasoning for (26) can be deduced using the cosine rule, see Fig. 5 for details. Since all MHC processes are i.i.d., the interference statistics are the same for each of the MHC processes (co-channel groups).

In order to analytically compute the expectation in (25), we follow the approximation in [13] where the MHC process is approximated as an inhomogeneous PPP that follows the conditional intensity of the MHC process. This approximation allows the use of the probability generating functional on \mathbb{R}^2 [3], which states that for a function $f: \mathbb{R}^2 \rightarrow [0, 1]$ the identity

$$\mathbb{E} \left[\prod_{x \in \Phi} f(x) \right] \equiv \exp \left(- \int_{\mathbb{R}^2} [1 - f(x)] \Lambda(dx) \right) \quad (27)$$

holds, where Φ is a PPP⁵ and $\Lambda(\cdot)$ is its intensity measure.

As the MHC point process features a strong dependency between its points, knowing that we have a serving BS u_o will influence the intensity of its surrounding region. This influence goes beyond just the interference protection zone $b(u_o, \delta)$ and causes an intensity reduction that gradually decays with distance. We can obtain this conditional intensity by adding two points in the parent PPP Φ_b with a known distance r ,

⁵In our case it is an inhomogeneous PPP approximating the MHC process under study. The probability generating functional is shown to hold well in the subsequent numerical examples.

$$\mathcal{L}_{I|R_o}(s) \approx \exp \left(- \int_{\delta}^{\infty} \int_{-\phi_o}^{\phi_o} [1 - \mathcal{L}_h(s(r^2 + R_o^2 + 2rR_o \cos \phi)^{-\frac{\alpha}{2}})] \lambda_b \frac{k(r)}{\rho} r \, d\phi dr \right), \quad (23)$$

where

$$\phi_o = \begin{cases} \pi - \cos^{-1} \frac{r}{2R_o} & : r < 2R_o \\ \pi & : \text{otherwise.} \end{cases} \quad (24)$$

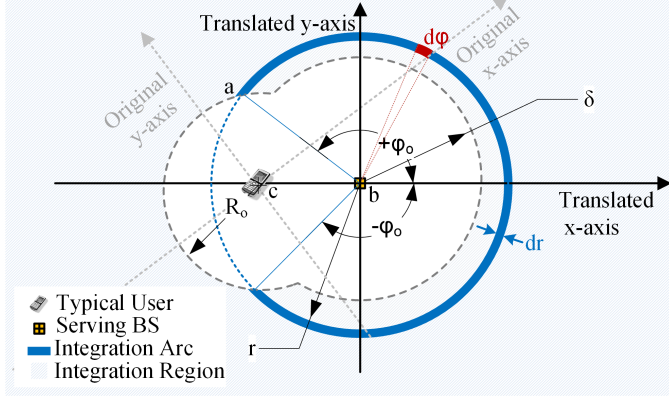


Fig. 5. The geometrical representation of the integration in (24), showing the integration arc extending from $-\phi_o$ to ϕ_o and the integration region. The original axis and the translated axis are indicated.

where we have shown in (7) that the Palm probability of having them both retained in the resulting MHC process is $k(r)$. Denote these two points as x_1 and x_2 with a distance $r = \|x_2 - x_1\|$. Further denote the event of x_1 to migrate to the MHC process as A , and the event of x_2 to migrate to the MHC process as B . Given a distance r , the following Bayesian rule applies

$$\mathbb{P}(B | A; r) = \frac{\mathbb{P}(A \cap B; r)}{\mathbb{P}(A)} = \frac{k(r)}{\rho}, \quad (28)$$

where we have $k(r) = \mathbb{P}(A \cap B; r)$ by definition, and $\mathbb{P}(A) = \rho$ is the probability for a point in the PPP to migrate to the MHC process by definition.

Coming back to the integration in (27), and considering a polar coordinate system (r, θ) , the conditional intensity can then be written as $\Lambda(rd\theta dr) = \lambda_b k(r) / \rho \, rd\theta dr$. As the parent PPP is isotropic, there is no dependency on the relative angle between two points in the MHC process [32].

We evaluate the double integral by translating the coordinate system with the origin at the serving BS and the typical user along the negative side of the x-axis. The translation significantly reduces the complexity of the numeric evaluation. Accordingly, the new coordinates r and ϕ respectively represent the distance and the angle between the interfering BSs and the serving BS. The infinitesimal integration arc is indicated in Fig. 5. Thus by substituting in (27) we obtain the result of Proposition 1. The angle limits of the integration in (24) are obtained using Euclidean reasoning as follows; from Fig. 5 we note that $\angle abc = \cos^{-1} \frac{r}{2R_o}$ using the cosine rule. Thus, $\pm\phi = \pi - \cos^{-1} \frac{r}{2R_o}$ for $r < 2R_o$. While in the case of $r \geq 2R_o$ the blue stripe extends to a full annulus and thus the integration limits will be $\phi = \pm\pi$ for $r \geq 2R_o$. \square

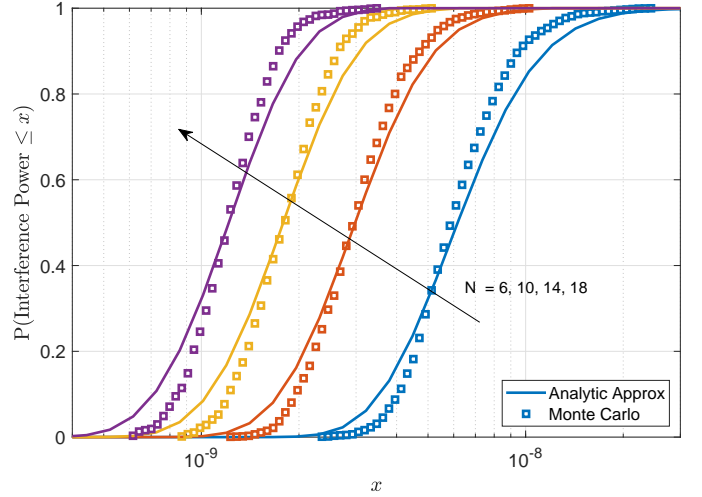


Fig. 6. The cumulative distribution function of the cellular interference using a constant BS density $\lambda_{\text{UMHC}} = \frac{2}{1000^2} \text{ m}^{-2}$, a variable number of frequency reuse groups $N = \{6, 10, 14, 18\}$, a path loss exponent $\alpha = 3$, a unit transmit power, and no channel fading ($h = 1$), the values of δ are obtained according to (15). The figure compares Monte-Carlo simulations with the analytic approximation in (29).

A numerical example is shown in Fig. 6 for a cellular network modeled using a UMHC process for a different number of stacked MHC processes $N = \{6, 10, 14, 18\}$ representing the number of frequency reuse groups. The overall cellular BS density is kept constant $\lambda_{\text{UMHC}} = \frac{2}{1000^2} \text{ m}^{-2}$, where a large value of the generating intensity is used $\lambda_b \rightarrow \infty$, thus the frequency reuse distance is calculated from (15). The CDF plot is obtained using numerical inversion of the Laplace transform and then a numerical expectation over the contact distance R_o , i.e.,

$$\begin{aligned} F_I(x) &= \mathbb{E}_{R_o} \left[\mathcal{L}^{-1} \left[\frac{1}{s} \mathcal{L}_{I|R_o}(s) \right] \right] \\ &= \int_0^{\infty} \mathcal{L}^{-1} \left[\frac{1}{s} \mathcal{L}_{I|r}(s) \right] f_{\text{UMHC}}(r) dr, \end{aligned} \quad (29)$$

where we utilize the convergence property of the UMHC process to a PPP in order to approximate the probability density function (PDF) of the contact distance as

$$f_{\text{UMHC}}(r) \approx 2\pi\lambda_{\text{UMHC}} r \exp(-\pi\lambda_{\text{UMHC}} r^2). \quad (30)$$

The results are compared to Monte-Carlo simulations, where the method of simulation is elaborated later on in Sec. VI-C.

VI. CELLULAR SUCCESS PROBABILITY

A. Analytical Formulation

A wireless transmission can be considered successful if the SINR at the receiver exceeds a certain threshold θ . Accord-

ingly, for a given BS-user distance R_o , we can express the link success probability as

$$\begin{aligned} p_L | h_o, R_o &= \mathbb{P}[\text{SINR} \geq \theta | h_o, R_o] \\ &= \mathbb{P}\left[\frac{h_o R_o^{-\alpha}}{I + W} \geq \theta | h_o, R_o\right] \\ &= F_{I|R_o}\left(\frac{h_o}{\theta R_o^\alpha} - W\right), \end{aligned} \quad (31)$$

where $F_{I|R_o}$ is the CDF of the aggregated interference I conditioned on the BS-user distance R_o and the fading of the desired BS-user link, while W is the average noise power normalized to the common transmit power of the BS. The random variable h_o models the fading of the serving BS channel. Accordingly, by deconditioning on h_o and R_o we can obtain the averaged performance of the cellular network as

$$\begin{aligned} p_s &= \mathbb{E}[p_L | h_o, R_o] = \mathbb{E}\left[F_{I|R_o}\left(\frac{h_o}{\theta R_o^\alpha} - W\right)\right] \\ &= \int_0^\infty \int_0^\infty F_{I|R_o}\left(\frac{h_o}{\theta R_o^\alpha} - W\right) \times f_{R_o}(r) f_{h_o}(u) dr du, \end{aligned} \quad (32)$$

where $f_{R_o}(r)$ and $f_{h_o}(v)$ are the PDFs of R_o and h_o respectively. The fading PDF can take any of the known models, e.g., Rayleigh, Rician, Nakagami, etc., while R_o follows the distribution of the UMHC point process. To illustrate the performance of a cellular network guarded with a frequency reuse distance, we depict in Fig. 7 a comparison between the success probability p_s against a varying threshold θ and for different reuse distances $\delta = \sqrt{\frac{N}{\pi \lambda_{\text{UMHC}}}}$ (see (15)). The analytical curves and Monte-Carlo simulations match to a good degree of accuracy, indicating the plausibility of approximating the MHC point process with an inhomogeneous PPP in Proposition 1. The simulation methodology is detailed Sec. VI-C.

B. Comparison with Experimental Data

As indicated in the literature review section, a plethora of previous works aimed at establishing an analytical approximation for frequency reuse in modern cellular networks. A popular method is to utilize a pool of N frequencies and assign these channels randomly to base stations [7], [33]. This method has a great advantage in simplifying the analytical study since when dealing with PPPs the randomly reduced set of PPP interferers is simply another PPP with a lower intensity. Indeed such method is very basic when compared to advanced interference mitigation schemes in cellular networks [34], and the performance of LTE-A and 5G networks is heavily dependent on these schemes. In fact, one of the main differentiators between network vendors is how well their interference mitigation is designed.

For comparing the ability of UMHC in capturing real network deployments we rely on publicly available data of a major telecom operator (Telstra) through the Australian Communication and Media Authority [35]. We select several subsets of this data trying to capture regions with relatively

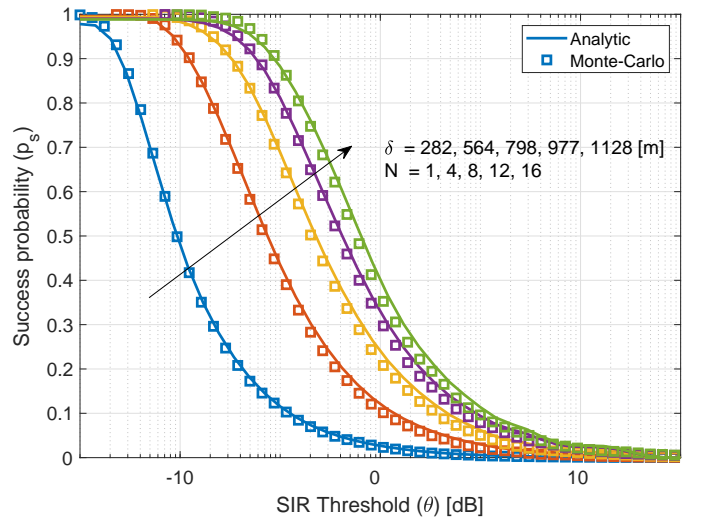


Fig. 7. The cellular success probability p_s versus the SINR threshold θ for a UMHC cellular model with different values of $N = \{1, 4, 8, 12, 16\}$. The generating parent PPPs has a very high density $\lambda_b \rightarrow \infty$, while the cellular density (UMHC density) is set to $\lambda_{\text{UMHC}} = \frac{1}{500 \times 500} \text{ m}^{-2}$. The noise power is ignored.

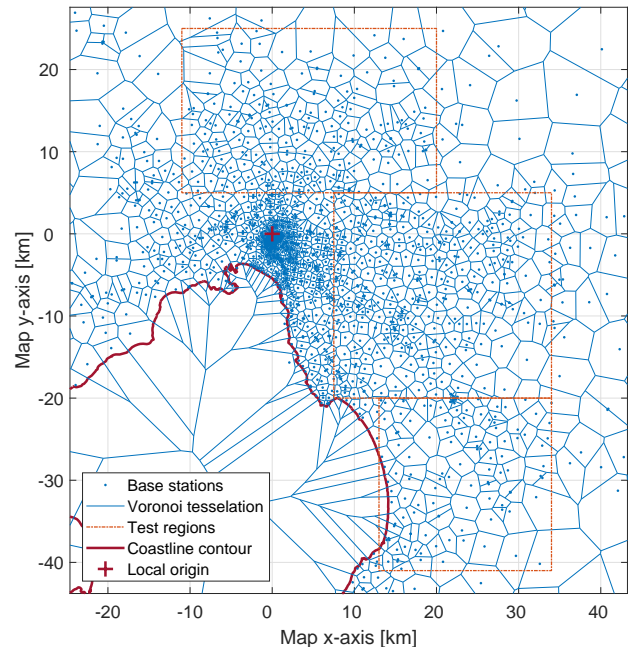


Fig. 8. The locations of base stations of a major telecom operator, indicating the test region used in the simulation. The location of base stations is sourced from the Australian Media and Communication Authority [35], coastline map is sourced from Geoscience Australia [36].

homogeneous density of BS as indicated in Fig. 8 showing the locations of the base stations⁶ and the associated Voronoi tessellation representing the serving cell of each base station. The total area of the three subsets is around 250 km², which makes our study statistically significant.

⁶It is noteworthy that in real-life scenarios, a telecom tower (or a *site*) usually consists of three directional sectors, where the presented model and analysis in this paper still apply to this case. In fact, it does not matter how many sectors each BS antenna is divided in. The distance to the serving BS remains unchanged, as do the distances to all interfering ones.

We compare the actual network deployment against two theoretical network layouts. In total the three scenarios are summarized below:

1) *UMHC Point Process (theoretical)*: In this method the reuse distance δ is calculated using (15) based on a given number of colors (frequency channels) N .

2) *Poisson Point Process with Random Coloring (theoretical)*: In this method a PPP network of base stations is created and the colors (frequency channels) are assigned randomly from a pool of colors having a cardinality of N . The analytical formulation of the probability of successful cellular service p_s is based on [18], where we invoke the *path loss-only scenario* in the comparison.

3) *Actual Network with Greedy Coloring (experimental)*: In this scenario the network is simulated for a different frequency reuse distances $\delta \in \{\delta_{\min}, \delta_{\max}\}$. For each of the simulated δ , a graph $G = (V, E)$ is constructed with the base stations as its vertices V , while the edges E are formed between base stations that are having distances below the reuse distance δ , i.e.,

$$E = \{(u, v) \in V : \|u - v\| \leq \delta\}. \quad (33)$$

After constructing the graph, it is colored using a fast greedy coloring algorithm [37] with repeated random sequences. Note that the ideal coloring might not be practically achievable in a reasonable simulation time, as coloring problems are known to be NP-hard. The resulting frequency plan using the selected greedy coloring algorithm is indeed suboptimal, however only very few residue base stations are given an extra frequency channel. We opt to ignore such group if the residue is less than 1% of the total number of base stations. The resulting number of colors N is recorded based on the given reuse distance δ . The entire simulation is extensively repeated (re-coloring) to obtain a statistically viable result, and we report both the mean performance and its standard deviation.

We quantify the performance in terms of the success probability p_s , which it is obtained against varying color numbers N (frequency channels) and compared in Fig. 9 for the three different scenarios; the theoretical models of (i) UMHC process and (ii) PPP, where both Monte-Carlo and analytical results show a good match and (iii) a practical network layout based on Telstra sites locations. It is interesting to observe that the average behavior of the practical network (scenario iii) becomes more aligned with the UMHC model as the number of frequency channels N increases, then it shows a good match for $N \geq 12$. The figure indicates a significant gap between the random frequency assignment in PPP and the UMHC model, which highlights the main added value of the proposed model showing its ability to accurately capture the performance of cellular networks when proper frequency assignment is utilized.

We note an interesting tendency of the practical network (Scenario iii) to follow the PPP model for a low number of frequency channels, i.e., $N \leq 6$. The intuition behind this is that the average number of sides (or neighbors) of a given Voronoi cell in the PPP process is 6, which means that it is significantly more likely to have at least one interfering neighbor when the available frequency channels $N \leq 6$. However, it is

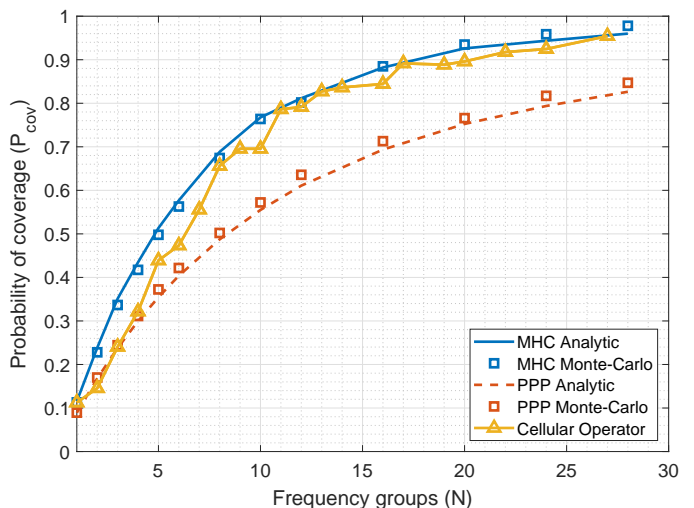


Fig. 9. The success probability of cellular network at SINR of $\theta = 10$ dB, comparing three scenarios: (i) UMHC point process (simulation and analytical), (ii) Randomly colored PPP (simulation and analytical) and (iii) a practical implementation of a cellular network.

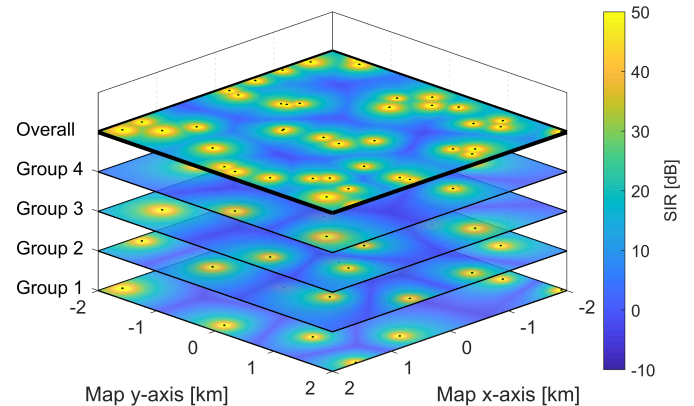


Fig. 10. A realization of UMHC process showing the SIR heatmap for each resource group MHC process, as well as the resulting combined heatmap of UMHC process (the top layer). Parameters $\lambda = \frac{1}{500 \times 500}$, $\delta = 800$ m.

important to know that a typical implementation of LTE/LTE-A system using 5, 10 MHz bandwidth will result in 25, 50 resource block (RB)⁷ respectively [1], i.e., $N = 25, 50$. Thus, the range of $N \geq 12$ in Fig. 9 is quite realistic to achieve in LTE/LTE-A and next-generation cellular technologies.

C. Simulation Methodology

In the previous sections we have compared the analytical results obtained by numerical integration with Monte-Carlo simulation to verify the consistency of the two approaches. The simulation is performed according to the following systematic steps:

⁷A resource block in LTE constitute the minimum possible resource assignment seen from the frequency domain perspective. Note that an LTE scheduler can assign multiple RBs simultaneously to users, thus the spectrum is usually divided disproportionately. As the proposed model is agnostic to the actual bandwidth of each resource group, it still applies for such a general case.

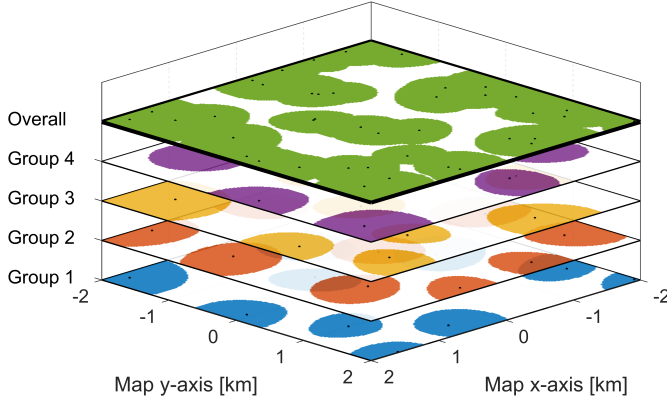


Fig. 11. The service area for each resource group MHC process, taking the SINR threshold as $\theta=10$ dB. The locations of BS are the same as Fig. 10.

Algorithm 1: Generate UMHC point process

```

1 Initialize the UMHC set  $\hat{\Xi} \leftarrow \emptyset$ 
2 for  $i = 1$  to  $N$  do
3   Generate a new PPP  $\hat{\Phi}_b$ 
4   Initialize the MHC set  $i$ ;  $\hat{\Phi}_i \leftarrow \emptyset$ 
5   for all  $x \in \hat{\Phi}_b$  do
6     Give a mark  $\mathcal{M}(x) = t \sim \mathcal{U}(0, 1)$ 
7   end
8   for all  $x \in \hat{\Phi}_b$  do
9     Build the set  $\hat{\Phi}_b \cap b(x, \delta)$ 
10    FLAG( $x$ )='Keep'
11    for all  $y \in \hat{\Phi}_b \cap b(x, \delta)$  do
12      if  $\mathcal{M}(x) > \mathcal{M}(y)$  then
13        FLAG( $x$ )='Remove'
14        Break
15      end
16    end
17    if FLAG( $x$ )=='Keep' then
18      Update the MHC set  $i$ ;  $\hat{\Phi}_i \leftarrow \hat{\Phi}_i \cup \{x\}$ 
19    end
20  end
21  Update the UMHC set  $\hat{\Xi} \leftarrow \hat{\Xi} \cup \hat{\Phi}_i$ 
22 end

```

- Generate a UMHC set $\hat{\Xi}$ using Algorithm 1 for a given δ
- Deploy UEs (sampling points) randomly inside the designated map region using a homogeneous intensity, while keeping a margin on the edges of the map to avoid the *edge-effect* resulting from the finite realization of the point process.
- For each user do the following:
 - Calculate the distance matrix between UEs and BSs as:

$$D = \left[\left(\mathbf{X}_{\text{UE}} \mathbf{J}_{1,m} - (\mathbf{X}_{\text{BS}} \mathbf{J}_{1,n})^T \right)^2 + \left(\mathbf{Y}_{\text{UE}} \mathbf{J}_{1,m} - (\mathbf{Y}_{\text{BS}} \mathbf{J}_{1,n})^T \right)^2 \right]^{1/2},$$

where n and m are the lengths of the Cartesian coordinate vector of the UEs and BSs respectively, and $\mathbf{X}_{\text{UE}}, \mathbf{Y}_{\text{UE}}$ and $\mathbf{X}_{\text{BS}}, \mathbf{Y}_{\text{BS}}$ are the coordinate column vector of UEs and BSs respectively, while $\mathbf{J}_{u,v}$ is the ones matrix of dimensions $u \times v$.

- Find the frequency channel of the serving BS
- At the user location, calculate the received powers from all BSs having the same frequency channel. The power is calculated using the power-law path loss equation and accommodating the fading factor.
- Sum the received power from all interfering BS and calculate the SINR accordingly.
- Append the SINR value to SINR vector $\hat{\gamma}$
- Obtain the empirical cumulative distribution function of the SIR vector $\hat{\gamma}$ conditioned on the given δ .
- The success probability is found by obtaining the empirical CDF of $\hat{\gamma}$, where $\hat{p}_s = 1 - \text{CDF}_{\hat{\gamma}}(\theta)$.

In Fig. 10 we visualize the concept of UMHC process (shown in the top layer) as a superposition of MHC processes (layers 1 to 4). The top layer represents the overall cellular network performance reported in terms of signal to interference ratio (SIR), while the lower layers represents the *logical* interference domains of the co-channel base stations.

VII. CONCLUSION

Based on an extensive comparison with a practical network deployment, it is clear that the union Matérn hard-core point process is capable of accurately capturing the effect of radio resource reuse in cellular networks. The accuracy of the UMHC process outperforms the random frequency assignment based on Poisson point process. The paper also shows how to construct a UMHC process and derive its pair correlation function as a measure of the point process regularity. In addition, the paper obtains the contact distance distribution for an arbitrary placed user towards the UMHC-modeled network. A generic analytic framework is presented that allows the numeric calculation of the interference statistics and accordingly the success probability under the interference-protection zone assumption. Future studies might investigate the superposition of other types of hard-core point processes.

REFERENCES

- [1] E. Dahlman, S. Parkvall, and J. Skold, *4G, LTE-Advanced Pro and the road to 5G*. Academic Press, 2016.
- [2] B. Błaszczyszyn, M. Haenggi, P. Keeler, and S. Mukherjee, *Stochastic geometry analysis of cellular networks*. Cambridge University Press, 2018.
- [3] M. Haenggi, *Stochastic geometry for wireless networks*. Cambridge University Press, 2012.
- [4] M. Z. Win, P. C. Pinto, and L. A. Shepp, "A mathematical theory of network interference and its applications," *Proceedings of the IEEE*, vol. 97, no. 2, pp. 205–230, 2009.
- [5] M. Di Renzo, A. Guidotti, and G. E. Corazza, "Average rate of downlink heterogeneous cellular networks over generalized fading channels: a stochastic geometry approach," *IEEE Transactions on Communications*, vol. 61, no. 7, pp. 3050–3071, 2013.
- [6] F. Baccelli and B. Błaszczyszyn, *Stochastic geometry and wireless networks: volume 1 theory*, ser. Foundations and Trends in Networking. Now Publishers Inc, 2010, vol. 3.
- [7] H. S. Dhillon, R. K. Ganti, F. Baccelli, and J. G. Andrews, "Modeling and analysis of K-tier downlink heterogeneous cellular networks," *IEEE Journal on Selected Areas in Communications*, vol. 30, no. 3, pp. 550–560, 2012.

- [8] R. K. Ganti and M. Haenggi, "Asymptotics and approximation of the SIR distribution in general cellular networks," *IEEE Transactions on Wireless Communications*, vol. 15, no. 3, pp. 2130–2143, March 2016.
- [9] N. Deng, W. Zhou, and M. Haenggi, "The Ginibre point process as a model for wireless networks with repulsion," *IEEE Transactions on Wireless Communications*, vol. 14, no. 1, pp. 107–121, Jan 2015.
- [10] I. Nakata and N. Miyoshi, "Spatial stochastic models for analysis of heterogeneous cellular networks with repulsively deployed base stations," *Performance Evaluation*, vol. 78, pp. 7–17, 2014.
- [11] K. Gulati, B. L. Evans, J. G. Andrews, and K. R. Tinsley, "Statistics of co-channel interference in a field of Poisson and Poisson-Poisson clustered interferers," *IEEE Transactions on Signal Processing*, vol. 58, no. 12, pp. 6207–6222, 2010.
- [12] X. Zhang and M. Haenggi, "A stochastic geometry analysis of inter-cell interference coordination and intra-cell diversity," *IEEE Transactions on Wireless Communications*, vol. 13, no. 12, pp. 6655–6669, Dec 2014.
- [13] M. Haenggi, "Mean interference in hard-core wireless networks," *IEEE Communications Letters*, vol. 15, no. 8, pp. 792–794, August 2011.
- [14] F. Baccelli, B. Blaszczyszyn, and P. Muhlethaler, "An ALOHA protocol for multihop mobile wireless networks," *IEEE Transactions on Information Theory*, vol. 52, no. 2, pp. 421–436, Feb 2006.
- [15] H. ElSawy and E. Hossain, "A modified hard core point process for analysis of random CSMA wireless networks in general fading environments," *IEEE Transactions on Communications*, vol. 61, no. 4, pp. 1520–1534, April 2013.
- [16] H. ElSawy, E. Hossain, and M. Haenggi, "Stochastic geometry for modeling, analysis, and design of multi-tier and cognitive cellular wireless networks: a survey," *IEEE Communications Surveys & Tutorials*, vol. 15, no. 3, pp. 996–1019, 2013.
- [17] M. Di Renzo, A. Guidotti, and G. E. Corazza, "Average rate of downlink heterogeneous cellular networks over generalized fading channels: a stochastic geometry approach," *IEEE Transactions on Communications*, vol. 61, no. 7, pp. 3050–3071, July 2013.
- [18] A. Al-Hourani and S. Kandeepan, "On modeling coverage and rate of random cellular networks under generic channel fading," *Wireless Networks*, vol. 22, no. 8, pp. 2623–2635, 2016.
- [19] H. ElSawy, A. Sultan-Salem, M. S. Alouini, and M. Z. Win, "Modeling and analysis of cellular networks using stochastic geometry: a tutorial," *IEEE Communications Surveys & Tutorials*, vol. 19, no. 1, pp. 167–203, Firstquarter 2017.
- [20] H. Nguyen, F. Baccelli, and D. Kofman, "A stochastic geometry analysis of dense IEEE 802.11 networks," in *IEEE INFOCOM 2007. 26th IEEE International Conference on Computer Communications*, May 2007, pp. 1199–1207.
- [21] G. Alfano, M. Garetto, and E. Leonardi, "New directions into the stochastic geometry analysis of dense CSMA networks," *IEEE Transactions on Mobile Computing*, vol. 13, no. 2, pp. 324–336, Feb 2014.
- [22] N. Deng, W. Zhou, and M. Haenggi, "Heterogeneous cellular network models with dependence," *IEEE Journal on Selected Areas in Communications*, vol. 33, no. 10, pp. 2167–2181, Oct 2015.
- [23] C. H. Lee and M. Haenggi, "Interference and outage in Poisson cognitive networks," *IEEE Transactions on Wireless Communications*, vol. 11, no. 4, pp. 1392–1401, April 2012.
- [24] N. Miyoshi and T. Shirai, "A cellular network model with Ginibre configured base stations," *Advances in Applied Probability*, vol. 46, no. 3, pp. 832–845, 2014.
- [25] H. Wei, N. Deng, W. Zhou, and M. Haenggi, "Approximate SIR analysis in general heterogeneous cellular networks," *IEEE Transactions on Communications*, vol. 64, no. 3, pp. 1259–1273, March 2016.
- [26] A. M. Ibrahim, T. ElBatt, and A. El-Keyi, "Coverage probability analysis for wireless networks using repulsive point processes," in *2013 IEEE 24th Annual International Symposium on Personal, Indoor, and Mobile Radio Communications (PIMRC)*, Sept 2013, pp. 1002–1007.
- [27] B. Matérn, "Spatial variation," *Meddelanden Fran Statens Skogsforskningsinstitut*, vol. 49, no. 5, 1960.
- [28] A. Al-Hourani, R. J. Evans, and S. Kandeepan, "Nearest neighbor distance distribution in hard-core point processes," *IEEE Communications Letters*, vol. 20, no. 9, pp. 1872–1875, Sept 2016.
- [29] S. N. Chiu, D. Stoyan, W. S. Kendall, and J. Mecke, *Stochastic geometry and its applications*. John Wiley & Sons, 2013.
- [30] R. K. Ganti and M. Haenggi, "Regularity in sensor networks," in *International Zurich Seminar on Communications*. IEEE, 2006, Conference Proceedings, pp. 186–189.
- [31] J. Abate and W. Whitt, "A unified framework for numerically inverting Laplace transforms," *INFORMS Journal on Computing*, vol. 18, no. 4, pp. 408–421, 2006.
- [32] J. Teichmann, F. Ballani, and K. G. van den Boogaart, "Generalizations of Matérn's hard-core point processes," *Spatial Statistics*, vol. 3, pp. 33–53, 2013.
- [33] J. G. Andrews, F. Baccelli, and R. K. Ganti, "A tractable approach to coverage and rate in cellular networks," *IEEE Transactions on Communications*, vol. 59, no. 11, pp. 3122–3134, 2011.
- [34] V. Pauli, J. D. Naranjo, and E. Seidel, "Heterogeneous LTE networks and inter-cell interference coordination," *Nomor Research GmbH*, pp. 1–9, 2010.
- [35] ACMA, "Australian Communications and Media Authority: register of radiocommunication licences." [Online]. Available: http://web.acma.gov.au/pls/radcom/site_proximity.main_page
- [36] Geoscience Australia, "Geodata coast 100k 2004." [Online]. Available: http://www.ga.gov.au/metadata-gateway/metadata/record/gcat_61395
- [37] A. Kosowski and K. Manuszewski, "Classical coloring of graphs," *Contemporary Mathematics*, vol. 352, pp. 1–20, 2004.



Akram Al-Hourani (M'10 SM'16) is a Senior Lecturer and telecommunication Program Manager at the School of Engineering, RMIT University. Before joining RMIT in 2016, he has been with The University of Melbourne as a Research Fellow. Dr Al-Hourani obtained his PhD in 2016 from RMIT University. Prior joining academia, Dr Al-Hourani had extensively worked in the ICT industry as an R&D engineer, radio network planning engineer and then as an ICT program manager for several projects spanning over different technologies; including mobile networks deployment, satellite networks, and railway ICT systems. Dr Al-Hourani was engaged in several research projects related to UAV communication networks, automotive radar, and the Internet of Things wireless networks. He published more than 43 journal articles and conference proceedings, including 3 book chapters. His current research interests include UAV communication systems, stochastic geometry, automotive radars, machine learning, and the Internet-of-Things over satellite.



Martin Haenggi (S'95–M'99–SM'04–F'14) received the Dipl.-Ing. (M.Sc.) and Dr.sc.techn. (Ph.D.) degrees in electrical engineering from the Swiss Federal Institute of Technology, Zurich (ETH), in 1995 and 1999, respectively. From 2007 to 2008, he was a Visiting Professor with the University of California at San Diego, and from 2014 to 2015, he was an Invited Professor with EPFL, Switzerland. He is currently the Freimann Professor of electrical engineering and a Concurrent Professor of applied and computational mathematics and statistics with the University of Notre Dame, Notre Dame, IN, USA. He is a coauthor of the monographs *Interference in Large Wireless Networks* (NOW Publishers, 2009) and *Stochastic Geometry Analysis of Cellular Networks* (Cambridge University Press, 2018) and the author of the textbook *Stochastic Geometry for Wireless Networks* (Cambridge, 2012), and has published 15 single-author journal articles. His scientific interests include networking and wireless communications, with an emphasis on cellular, amorphous, ad hoc (including D2D and M2M), cognitive, and vehicular networks. Dr. Haenggi served as a Steering Committee Member of the IEEE Transactions on Mobile Computing (TMC), and the Chair of the Executive Editorial Committee of the IEEE TWC. He also served as a Distinguished Lecturer for the IEEE Circuits and Systems Society, a TPC Co-chair for the Communication Theory Symposium of the 2012 IEEE International Conference on Communications (ICC'12), the 2014 International Conference on Wireless Communications and Signal Processing (WCSP'14), and the 2016 International Symposium on Wireless Personal Multimedia Communications (WPMC'16). For both his M.Sc. and Ph.D. theses, he was awarded the ETH medal. He also received a CAREER Award from the U.S. National Science Foundation, in 2005, and three awards from the IEEE Communications Society, the 2010 Best Tutorial Paper award, the 2017 Stephen O. Rice Prize Paper Award, and the 2017 Best Survey Paper Award. He served as an Associate Editor of the *Journal of Ad Hoc Networks* (Elsevier), the *IEEE Transactions on Mobile Computing (TMC)*, the *ACM Transactions on Sensor Networks*, a Guest Editor for the *IEEE Journal on Selected Areas in Communications*, the *IEEE Transactions on Vehicular Technology*, and the *EURASIP Journal on Wireless Communications and Networking*. From 2017 to 2018, he was the Editor-in-Chief of the TWC. He was a 2017 and 2018 Clarivate Analytics Highly Cited Researcher.